Design and Implementation of a Range-Based Formation Controller for Marine Robots

Jorge M. Soares[1,3], A. Pedro Aguiar[1,2],
António M. Pascoal[2], and Alcherio Martinoli[3]

[1] Laboratory of Robotics and Systems in Engineering and Science, Instituto Superior Técnico, Technical University of Lisbon, Av. Rovisco Pais, 1049-001 Lisboa, Portugal.
[2] Department of Electrical and Computer Engineering, Faculty of Engineering, University of Porto, Rua Dr. Roberto Frias, 4200-465 Porto, Portugal.
[3] Distributed Intelligent Systems and Algorithms Laboratory, School of Architecture, Civil and Environmental Engineering, École Polytechnique Fédérale de Lausanne (EPFL), CH-1015 Lausanne, Switzerland.

Abstract. There is considerable worldwide interest in the use of groups of autonomous marine vehicles to carry our challenging mission scenarios, of which marine habitat mapping of complex, non-structured environments is a representative example. Relative positioning and formation control becomes mandatory in many of the missions envisioned, which require the concerted operation of multiple marine vehicles carrying distinct, yet complementary sensor suites. However, the constraints placed by the underwater medium make it hard to both communicate and localise the vehicles, even in relation to each other, let alone maintain them in a formation. As a contribution to overcoming some of these problems, this paper deals with the problem of keeping an autonomous marine vehicle in a moving triangular formation with respect to two leader vehicles. Simple feedback laws are derived to drive a controlled vehicle to its intended position in the formation using acoustic ranges obtained to the leading vehicles with no knowledge of the formation path. The paper discusses the implementation of this solution in the MEDUSA class of autonomous marine vehicles operated by IST and describes the results of trials with these vehicles exchanging information and ranges over an acoustic network.

1 Introduction

The last two decades have witnessed tremendous progress in the development of marine technologies that are steadily affording scientists and commercial companies advanced equipment and methodologies for ocean exploration and exploitation. Recent advances in robotics, sensors, computers, communications and information systems are being brought to bear on the development of sophisticated technologies to enable safer, better, faster, and more efficient methodologies for ocean exploration. These advances will undoubtedly revolutionise the way the oceans are studied, effectively placing scientists at the threshold of a new and exciting area when science and technology will join efforts to unravel the secrets

behind recent and unexpected discoveries: intriguing ecosystems and life forms, thermal vents and cold seeps, and huge accumulations of methane in the form of gas hydrates, to name but a few. New technologies, especially autonomous marine robots capable of roaming the oceans freely, equipped with advanced sensor suites for data collection at an unprecedented scale, will also play a key role in the related fields of marine archaeology, harbour security, and transportation. Advanced marine robotic systems are also expected to afford commercial operators new tools to drastically improve the means available to monitor critical infrastructures and ocean energy production facilities (e.g. wave and wind energy generation plants), assess the size and type of fish stocks, detect and monitor the effect of hydrocarbon spills, assess the extent of mineral, oil, and gas deposits, carry out and monitor the impact of underwater mining activities, and increase the efficiency and safety of gas and oil exploration and exploitation activities. Recent developments in the field of autonomous marine vehicles, with increasingly powerful and affordable vehicles coming on the market, are steadily paving the way for a multitude of novel applications.

Many tasks envisioned to be within the reach of multi-AUV (Autonomous Underwater Vehicle) groups require the vehicles to work cooperatively. That often translates to being able to move in formation, i.e. while maintaining their relative positions. This paper considers the problem of triangular formation keeping under severe communication and localisation constraints, conditions typically found when working with groups of AUVs, and summarises the work that was previously published in [1, 2]. For a reference scenario consisting of two localised leader vehicles on the surface and an underwater follower vehicle, we use acoustic ranging and communications to establish and maintain a moving formation of the three vehicles. Of the multiple real-world applications matching this scenario, a typical one is surface-guided underwater exploration. We make a realistic assumption that the AUV has independent depth control, and focus on formation control in the 2D plane only.

We propose a control strategy that estimates the formation speed and heading from the acoustic ranges obtained to the two leading vehicles, and uses simple feedback laws for speed and heading to drive suitably defined common and differential errors to zero. We then discuss the implementation of this solution in a MEDUSA-class autonomous marine vehicle, describing the challenges posed by the medium and the changes that arise as a consequence, and present the results of real world tests performed with 3 autonomous vehicles.

The paper is organised as follows: the present section provides important background to our work and Section 2 summarizes previous related work; Section 3 describes the specific problem in more detail; Section 4 contains a description of the MEDUSA class of autonomous marine vehicles and their dynamic models; Section 5 describes the error dynamics and outlines the control laws for vehicle heading and linear velocity; Section 6 discusses the necessary adaptations for implementation in a real vehicle and Section 7 summarises the results obtained during real-world trials with 3 autonomous marine vehicles. Finally, Section 8 contains the conclusions and lists directions for future research.

2 Related work

One interesting work in formation control for mobile robots is described in [3], where the authors discuss approaches for both range-bearing and range-range control, depending on the available sensors, to solve a leader-follower control problem for a formation graph with an arbitrary number of vehicles; in both cases, knowledge of the leader motion is assumed. In [4], and supported by robot experiments, a different graph-based leader-follower solution using range and bearing is proposed. Another strategy is described in [5] for a 4-vehicle station keeping problem, using exclusively range measurements and holonomic vehicles described by simple kinematic points. In [6], a similar scenario is considered, although global convergence is only proved for a triangular formation.

Bearing-only methods are also available for square [7] and triangular [8, 9] formations. In [10], the authors advance algorithms to coordinate a formation of mobile agents when the agents can only measure the ranges to their immediate neighbours. This solution requires that subsets of non-neighbouring agents localise the relative positions of their neighbours while these are stationary, and then move to minimise a cost function.

For the special case of marine vehicles, a solution that decouples the controllers for formation shape, formation motion and vehicle orientation, but requires position information is proposed in [11]. Coordinated path following approaches are presented in [12] and [13], the latter specifically dealing with underwater pipeline inspection. These strategies assume that the path to be followed is known to all vehicles, and generally work by exchanging some along-path synchronisation measure. An example of a real-world AUV operation making use of formation control is documented in [14].

3 Problem statement

Figure 1 illustrates the control problem discussed in this paper, and shows two leading vehicles (vehicles 2 and 3, represented as x_2 and x_3) moving along a certain unknown path, and a follower (vehicle 1, represented as x), of which we have control. Through the remainder of this paper, and unless otherwise stated, the absence of an index indicates a variable or parameter related to vehicle 1, the controlled or trailing vehicle.

The goal is for the trailing vehicle to follow the leaders in an equilateral triangular formation of side d, i.e. in the figure, x should converge to the desired position x_d. There exists a symmetric solution to the problem, with the desired position x_d mirrored in relation to the segment defined by $x_2\, x_3$. The solution shown in Fig. 1 corresponds to a *following motion* and the mirrored solution to a *leading motion*. We only deal with the case of following motion.

The basic control problem consists, as we have seen, of deriving control laws to drive x to x_d. The challenge stems from working with AUVs with no access to global localisation methods and with slow and unreliable inter-vehicle communication. Here, we make a reasonable assumption that the only localisation

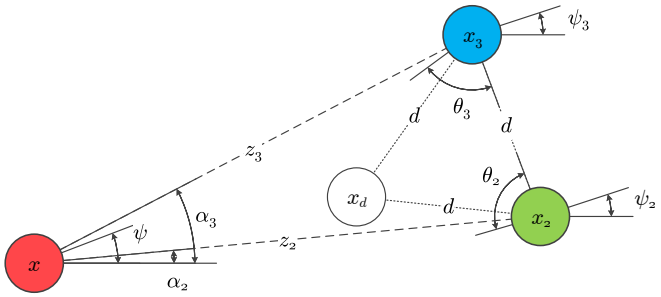

Fig. 1. System of three robots (x, x_2, x_3) and their intended triangular formation (x_d, x_2, x_3). The image shows many of the relevant parameters, including the formation and independent vehicle headings, as well as the relationships (ranges and bearings) between them. The heading and course of the vehicles are only aligned in the absence of current. Note that the colour convention holds throughout the paper.

hardware available on the AUV is a low data rate acoustic modem and ranging device, which is the case for our vehicles, presented in the next section. The complete problem becomes, then, to derive and implement control laws that achieve convergence of x to x_d using only limited communication and information.

4 Vehicle details

The MEDUSA-class autonomous semi-submersible robotic vehicles, shown in Fig. 2, were developed at the Laboratory of Robotics and Systems in Engineering and Science (LARSyS), Instituto Superior Técnico. The MEDUSAs were originally designed and built as surface vehicles, but a diving capable version is now also operational. Nevertheless, in this paper we use an artificially constrained surface-bound MEDUSA to emulate our AUV. This has some practical advantages, as we can mimic the most relevant characteristics of an AUV while retaining a GPS receiver and a radio communication channel, respectively used for ground truth and remote monitoring (but not for communication with the remaining vehicles).

Each MEDUSA-class vehicle weighs approximately 30 Kg and consists of two longitudinal acrylic housings with a total length of around 1 m. The upper body is partially above the surface and carries an EPIC single-board computer, an RTK-enabled GPS receiver, a full navigation sensor suite and an underwater camera. Most of the lower body is taken up by the batteries. An 802.11 interface is used for surface communications, while a Tritech acoustic modem enables underwater communication. The vehicle is propelled by two side-mounted, forward-facing stern thrusters that directly control surge and yaw motion, and is capable of speeds up to 1.5 m/s.

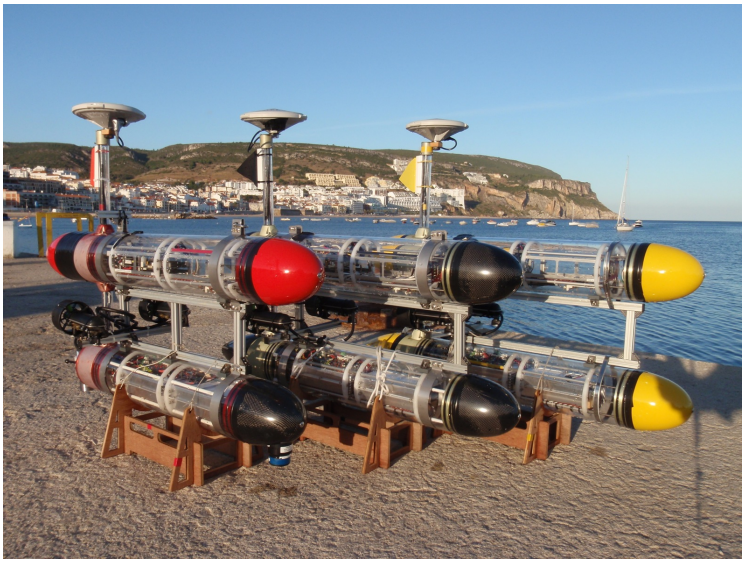

Fig. 2. The MEDUSA AMVs being readied for deployment at an experimental site.

As the vehicle moves on the surface, its kinematic equations take the form

$$\begin{aligned}\dot{x} &= u\cos\psi - v\sin\psi \\ \dot{y} &= u\sin\psi + v\cos\psi \\ \dot{\psi} &= r,\end{aligned}$$

where u (surge speed) and v (sway speed) are the body axis components of the velocity of the vehicle, x and y are the Cartesian coordinates of its centre of mass, ψ defines its orientation (heading angle), and r its angular velocity. The motions in heave, roll and pitch can be neglected, due to the large enough metacentric height. The resulting dynamic equations of motion for surge, sway and yaw are

$$\begin{aligned}m_u\dot{u} - m_v vr + d_u u &= \tau_u \\ m_v\dot{v} + m_u ur + d_v v &= 0 \\ m_r\dot{r} - m_{uv}uv + d_r r &= \tau_r,\end{aligned}$$

where τ_u stands for the external force in surge (common mode), τ_r for the external torque (differential mode), and the m and d terms represent vehicle masses, hydrodynamic added masses, and linear and quadratic hydrodynamic damping effects. The complete model for the MEDUSA vehicles is presented in [15].

5 Controller design

We start by deriving the control strategy using a basic kinematic model for the vehicles (distinct from the realistic model found in the previous section), and under the assumption of continuous communication and control. While the resulting controllers are not guaranteed to apply in the real world, we later show that, with the proper adaptations, they do indeed work on the real vehicles.

We assume that the follower starts from a following position, in order to converge to a following motion, and that the leader vehicles (2 and 3) move at a distance d from each other, according to simple kinematics described by

$$\dot{x}_i = \begin{bmatrix} v_i \cos\psi_i \\ v_i \sin\psi_i \end{bmatrix}, \quad i = 2, 3$$

where $(v_2 + v_3)/2 = v_f$ is the formation speed. The control signals are the linear velocity v and the heading ψ, and the kinematic model of the follower is given by

$$\dot{x} = \begin{bmatrix} v \cos\psi \\ v \sin\psi \end{bmatrix},$$

where $x \in R^2$ denotes its Cartesian position. Here, we accept that both leaders move with a common heading $\psi_f = \psi_2 = \psi_3$, and that the total velocity vector of each leading vehicle is always perpendicular to the line segment that joins them. The heading ψ_f is unknown to vehicle 1.

Separate controllers are designed to stabilise each error measure, with the speed controller stabilising the common mode error and the heading controller stabilising the differential mode error. What follows is an overview of the resulting controllers; intermediate steps in the derivation and proofs of convergence can be found in [1].

5.1 Error dynamics

Let $z_i = \|x_i - x\|; i = 2, 3$ denote the distances from the trailing vehicle to each of the leaders. From the range measurements, we define the common and differential mode errors

$$\epsilon = \frac{e_2 + e_3}{2} = \frac{z_2 + z_3}{2} - d$$
$$\delta = e_3 - e_2 = z_3 - z_2,$$

respectively with $e_i = z_i - d; i = 2, 3$. From the definition of z_i, it follows that

$$\dot{z}_i = v_i \cos(\alpha_i - \psi_f) - v \cos(\alpha_i - \psi),$$

Although the control strategy can be applied to other types of trajectories, the next sections assume the simpler case of straight line constant-speed motion for

the two leading vehicles. This means that $v_2 = v_3 = v_f$ and the simplified error dynamics for ϵ and δ become

$$\dot{\epsilon} = \cos\beta \left(v_f \cos\varphi - v \cos(\varphi + \tilde{\psi}) \right) \tag{1}$$

$$\dot{\delta} = 2 \sin\beta \left(v_f \sin\varphi - v \sin(\varphi + \tilde{\psi}) \right),$$

where

$$\beta = \frac{\theta_2 + \theta_3}{2} - \frac{\pi}{2}$$
$$\varphi = \frac{\theta_2 - \theta_3}{2},$$

and $\tilde{\psi} = \psi_f - \psi$ is the heading error.

5.2 Speed controller

We propose the following speed controller to regulate the common mode error ϵ to zero:

$$v = K_p^s \epsilon + K_i \int_0^t \epsilon \, d\tau,$$

where $K_p^s > 0$ and $K_i > 0$ are the proportional and integral gains, respectively. The rationale behind the proposed control law is that when the leader vehicles follow a straight-line trajectory with constant speed v_f, $\psi = \psi_f$ and $\delta = 0$ (i.e. x is on the perpendicular bisector of the x_2x_3 line segment), the dynamics of ϵ in (1) reduce to

$$\dot{\epsilon} = \cos\beta(v_f - v),$$

and, since $\cos\beta > 0$, a control law $v = v_f + K_p^s \epsilon$, $K_p^s > 0$ stabilises exponentially the origin $\epsilon = 0$, provided β does not converge to $-\frac{\pi}{2}$. As v_f is unknown, we include an integral term to learn it.

5.3 Heading controller

For the heading controller we propose the following control law that uses the differential mode error δ:

$$\psi = \hat{\psi}_f + \gamma(K_p^h \delta),$$

where $K_p^h > 0$, $\hat{\psi}_f$ denotes an estimate of the formation heading ψ_f, and γ is any function such that $\sin(\gamma(ay))y > 0, \forall a > 0$. An example is the saturation function $\gamma(y) = \frac{\pi}{2}\,\mathrm{sat}(y)$.

6 Implementation

While the controllers developed show good performance under the assumptions made during their derivation (results in [1]), moving to a real-world implementation requires significant changes.

First and foremost, ranges in an underwater setting are most often measured using acoustic equipment, by registering the time of flight of an echo request and reply. In our case, the ranging is done by the general purpose Tritech acoustic modem that equips the MEDUSA. The low transmission speed makes it so that we can only issue one echo request every few seconds. Since transmissions cannot overlap on the single common channel, time multiplexing must be used to obtain the ranges to each of the leader vehicles. We choose to query each one separately, although other solutions are possible, e.g. emitting a broadcast ping with vehicle-dependent delayed replies. Since both leaders have to be queried, a complete information update only occurs every four seconds. This is in stark contrast with our previous assumption of continuous measurement.

To prevent changes to the algorithms, we have chosen to implement two hybrid Kalman filters that take the discrete samples and output a continuous estimate of the distances. The range information received is never current, and comes with a latency of approximately 0.5 seconds, imposed by transmission times and I/O scheduling on both the sender and receiver. We decided not to implement any mitigation techniques (e.g. back-dating the filter updates), instead retaining the simplicity of the solution.

The measurements taken are inherently noisy. This noise is, for practical purposes, quite low - we did not fully characterise it, but the individual ranging error was predominantly under 0.5 m - but it again must be taken into account. The same way, outliers are inevitable, albeit infrequent. These are mostly caused by floor geometry and non-uniform propagation in the water, leading to the reception of an echo reply through a path other than the shortest one and resulting in an overestimation of the distance. We implemented a simple outlier filter based on a sliding window. Losses are also an inescapable reality, and need to be tolerated within reasonable limits.

The heading for the leaders, despite being used, is also not implicitly available to the follower, and has to be communicated. Seeing as the vehicles use full-featured acoustic modems to measure ranges, it is possible to piggyback data on the ranging reply. This feature must be used with caution, in order not to over-extend communication times (thereby decreasing the sampling rate even further), but adding an integer to the reply is without major consequences. In our implementation, the heading is transmitted as a piggybacked single byte on the echo reply, and fed to another hybrid Kalman filter with the incoming values whenever a new range is received. While each range estimator is, in the absence of losses, updated every four seconds, the heading estimator is updated every two seconds. As the heading of both vehicles should be close to and converge to the formation heading, this allows for a higher quality and more responsive estimate.

An overview of the resulting implementation is presented in Fig. 3. The expressions for the speed and heading controller in our implemented solution remain unchanged, with the required adaptations being handled by earlier stages. While we are using a surface vehicle, the solution is applicable for constant-depth underwater operations and, with minor changes, to variable-depth underwater vehicles equipped with a depth sensor and independent depth control.

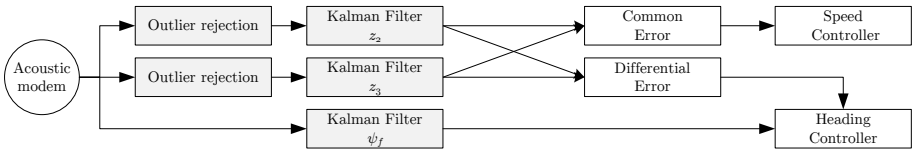

Fig. 3. Structure and data flow in the MEDUSA implementation of the formation control algorithm. Modules in grey perform the conversion of available discrete data to the continuous signals required the algorithm.

7 Experimental evaluation

Real world trials were conducted in June 2012 at Parque das Nações in Lisbon, Portugal. This is a fairly sheltered saltwater bay connected to the Tagus estuary, of which an aerial view is presented in Fig. 4. It provides for ample space for testing, with minimal currents and good conditions for deployment of the control center. Water depth is restricted (generally under 5 m), which limits the performance of the acoustic communication systems. All vehicles were equipped with the full sensor suite, including RTK GPS, but the trailing vehicle only logs the position data for ground truth and does not use it, in any way, for navigation.

The leader vehicles, running the Coordinated Path Following algorithm described in [15], were configured to execute the 3-legged lawnmower manoeuvre presented below, spanning around 120 m x 120 m, at a reference speed $v_f = 0.4\,\mathrm{m/s}$. The vehicles were set to a triangular formation with $d = 13\,\mathrm{m}$.

Figure 5 shows a top view of the paths described by the three vehicles, starting in the upper right corner: the leaders are pictured in green and blue, with the red follower trailing behind. A transient can be noticed at the beginning: none of the vehicles start in their designated position or heading and need to adjust. The movement of the leader and their rapidly varying reported headings impact the Kalman filter estimate, causing the controlled vehicle to start in a non-ideal direction. Afterwards, the leaders negotiate the set path while the follower accurately position in the formation.

Minimal packet loss was observed during the trials. When it takes place, it is mostly while turning, presumably due to mis-alignment of the acoustic modems in the three vehicles, and is the leading factor causing the vehicle to stray off path. Nevertheless, Fig. 6 shows that the errors are low: after the initial

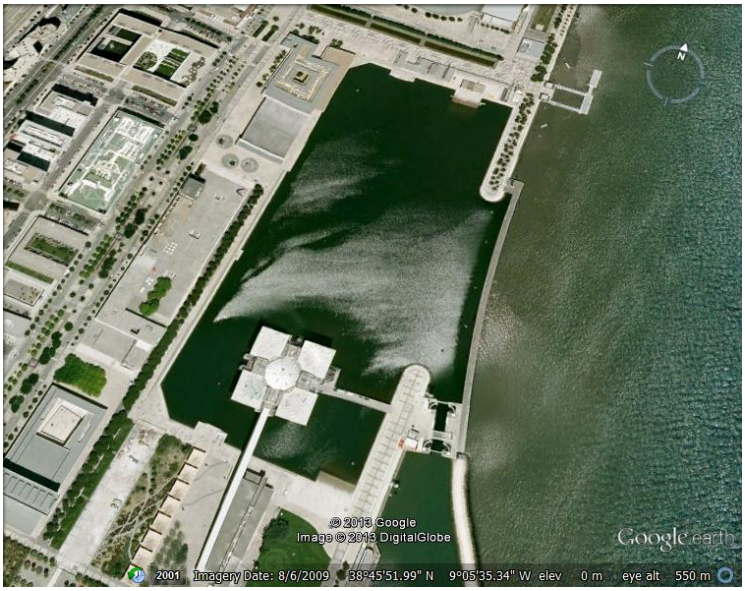

Fig. 4. Aerial view of the sheltered salt-water bay in the Tagus river estuary where the tests were conducted.

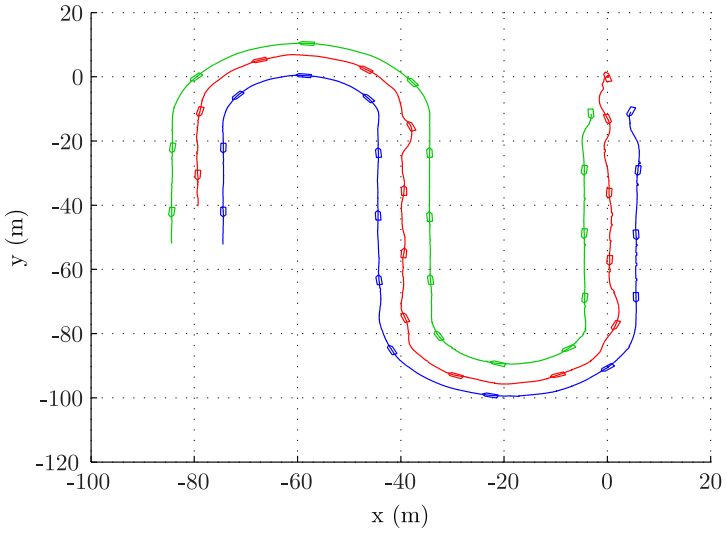

Fig. 5. Path followed by the vehicles during real-world trials. The manoeuvre starts on the top right corner, and the trajectory of the controlled vehicle is shown in red.

adjustment period, the common mode error generally remains under 1 m, and the differential mode error remains under 3 m. Two minor peaks in the common error, caused by packet loss, can be seen around 180 s and 400 s, at the beginning of each turn.

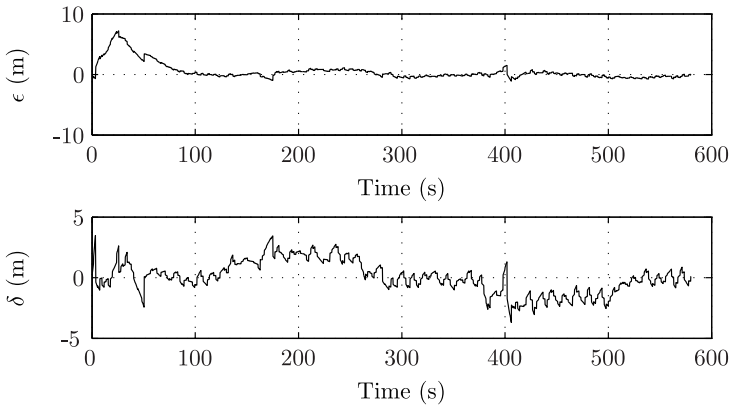

Fig. 6. Time evolution of the common mode and differential mode errors along the lawnmower path.

Figure 7 shows the speed of the follower (the mean speed of the leaders is, as previously stated, 0.4 m/s), as well as the headings of the follower (red) and leaders (green and blue). It also shows the received heading packets from the leader, represented by the black dots. As expected, the plots closely match the error plots, with a clearly visible peak in speed at 400 s.

8 Conclusions and outlook

In this paper we reviewed a solution to a three-vehicle formation keeping problem where a follower moves in a triangular formation behind two leading vehicles, using inter-vehicle range measurements with no a priori knowledge of the path taken by the leaders. The algorithm considers a discrete and noisy measurement model with low sampling rate and uses additional heading information piggybacked on the acoustic echo reply.

The proposed solution was implemented and tested on the MEDUSA class of vehicles. The evaluation results show good performance, with minimal disturbance under straight lines, even in the presence of packet loss, sensor noise and outliers. The hybrid Kalman filters used are able to accurately estimate the distances, despite the low rate of the acoustic ranges, and the piggybacked heading information allows for smooth response to changes in direction.

Work is ongoing regarding the testing of the algorithm on an underwater setting, using a new diving version of the MEDUSA. The algorithm is also being

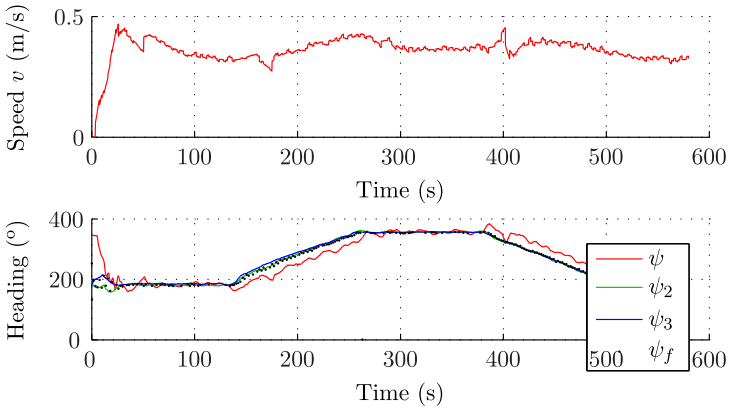

Fig. 7. Time evolution of the follower vehicle speed v, and headings ψ, ψ_2, ψ_3, as well as the discrete references received acoustically, ψ_f. The vehicle speed is estimated from GPS measurements, and has non-negligible associated noise.

extended to a larger number of vehicles and different formation shapes. Future work should include the pairing of the algorithm with robust methods for initialisation and collision avoidance. Finally, open sea trials will allow us to test and validate the algorithm in the presence of stronger currents, waves and winds.

9 Acknowledgements

This work was supported by projects CONAV/FCT-PT [PTDC / EEACRO / 113820 / 2009], MORPH [EU FP7 ICT 288704], and FCT [PEst-OE / EEI / LA0009 / 2013]. Partially funded with grant SFRH / BD / 51073 / 2010 from Fundação para a Ciência e Tecnologia.

References

1. Soares, J.M., Aguiar, A.P., Pascoal, A.M.: Triangular formation control using range measurements : an application to marine robotic vehicles. In: IFAC Workshop on Navigation, Guidance and Control of Underwater Vehicles (NGCUV2012), Porto, Portugal (2012)
2. Soares, J.M., Aguiar, A.P., Pascoal, A., Martinoli, A.: Joint ASV/AUV Range-Based Formation Control: Theory and Experimental Results. In: 2013 IEEE International Conference on Robotics and Automation, Karlsruhe, Germany (2013)
3. Desai, J., Ostrowski, J., Kumar, V.: Modeling and control of formations of nonholonomic mobile robots. Robotics and Automation, IEEE Transactions on **17**(6) (2001) 905–908
4. Falconi, R., Gowal, S., Martinoli, A.: Graph-based distributed control of non-holonomic vehicles endowed with local positioning information engaged in escorting missions. In: 2010 IEEE International Conference on Robotics and Automation, Anchorage, Alaska, USA, IEEE (May 2010) 3207–3214

5. Cao, M., Morse, A.S.: Station keeping in the plane with range-only measurements. In: 2007 American Control Conference, New York, NY, USA, IEEE (July 2007) 5419–5424
6. Oh, K.K., Ahn, H.S.: Formation control of mobile agents based on inter-agent distance dynamics. Automatica **47**(10) (October 2011) 2306–2312
7. Bishop, A.N.: Distributed bearing-only formation control with four agents and a weak control law. In: 2011 9th IEEE International Conference on Control and Automation (ICCA), Santiago, Chile, IEEE (December 2011) 30–35
8. Bishop, A.N.: A Very Relaxed Control Law for Bearing-Only Triangular Formation Control. In: Proceedings of the 18th IFAC World Congress, Milano, Italy (August 2011) 5991–5998
9. Basiri, M., Bishop, A.N., Jensfelt, P.: Distributed control of triangular formations with angle-only constraints. Systems & Control Letters **59**(2) (February 2010) 147–154
10. Cao, M., Yu, C., Anderson, B.D.O.: Formation control using range-only measurements. Automatica **47**(4) (April 2011) 776–781
11. Yang, H., Zhang, F.: Geometric formation control for autonomous underwater vehicles. In: 2010 IEEE International Conference on Robotics and Automation, Anchorage, Alaska, USA, IEEE (May 2010) 4288–4293
12. Ghabcheloo, R., Aguiar, A.P., Pascoal, A.M., Silvestre, C., Kaminer, I., Hespanha, J.: Coordinated path-following in the presence of communication losses and time delays. SIAM Journal on Control and Optimization **48**(1) (2009) 234
13. Xiang, X., Jouvencel, B., Parodi, O.: Coordinated Formation Control of Multiple Autonomous Underwater Vehicles for Pipeline Inspection. International Journal of Advanced Robotic Systems **7**(1) (2010) 1
14. Leonard, N.E., Paley, D.A., Lekien, F., Sepulchre, R., Fratantoni, D.M., Davis, R.E.: Collective Motion, Sensor Networks, and Ocean Sampling. Proceedings of the IEEE **95**(1) (January 2007) 48–74
15. Ribeiro, J.: Motion Control of Single and Multiple Autonomous Marine Vehicles. Master's thesis, Instituto Superior Técnico - Technical University of Lisbon (2011)